

# **Environmental Geotechnics**

# Grading curve relations for saturated hydraulic conductivity of granular materials

ENGE-2023-131-R2 | Paper

Submitted on: 22-11-24

Submitted by: Emőke Imre, Zsombor Illes, Francesca Casini, Giulia Guida, Shuyin Feng, Maria Datcheva, Wiebke Baille, Agnes Balint, Delphin Kabey, Janos Lorincz, James Leak, Daniel Barreto

Keywords: GRANULAR MATERIALS, PERMEABILITY & PORE-RELATED PROPERTIES, STATISTICAL ANALYSIS

PDF auto-generated using **ReView** from



#### **Editorial Panel comments - Author's reply**

Many thanks to the Editor for the latest review. It includes the single comment below:

1. Table citation number of A2-1 is incorrect. Please do the corrections.

Response:

Many thanks for pointing this out. The reference has now been corrected to Table A2-1.

- Article type: Paper
- Date text revised: 20/06/2024

\_\_\_\_\_

- Number of words in main text and tables: 5000 app: 733
- Number of figures: 10 + 2 in appendices

Grading curve relations for saturated hydraulic conductivity of granular materials

#### Author 1

- Emoke Imre, Ph.D., Habil
- Bánki Donát Faculty of Mechanical and Safety Engineering and EKIK HBM Research Centers, Óbuda University, Budapest Hungary
- orcid.org/0000-0001-6746-027X

Author 2

- Zsombor Illés, M.Sc.
- Department of Engineering Geology and Geotechnics, Budapest University of Technology and Economics, Budapest, Hungary
- <u>orcid.org/0000-0001-9351-1763</u>

Author 3

- Francesca Casini, Ph.D.
- Department of Civil Engineering and Informatics, Università degli studi di Roma Tor 33Vergata, Rome, Italy
- <u>orcid.org/0000-0001-7933-9055</u>

Author 4

- Giulia Guida, Ph.D.
- Department of Civil Engineering and Informatics, Università degli studi di Roma Tor Vergata, Rome, Italy
- orcid.org/0000-0003-1129-7906

Author 5

- Shuyin Feng, Ph.D.
- Department of Civil Engineering, Birmingham City University, UK
- <u>orcid.org/0000-0002-3837-6762</u>

#### Author 6

- Maria Datcheva, Ph.D.
- Institute of Mechanics and Institute of Information and Communication Technologies, Bulgarian Academy of Sciences, Sofia, Bulgaria
- orcid.org/0000-0002-0801-4795

Author 7

- Wiebke Baille, Ph.D.
- Ruhr-Universität Bochum, Bochum, Germany
- orcid.org/0000-0001-6852-9427

Author 8

- Ágnes Bálint, Ph.D., Habil
- Óbuda University, Institute of Environmental Engineering and Natural Sciences, Budapest, Hungary
- orcid.org/0000-0003-3527-6835

Author 9

- Delphin Kabey Mwinken
- AIAM Doctoral School, Óbuda University, Hungary
- <u>orcid.org/0000-0002-2540-9027</u>

Author 10

- János Lorincz
- AIAM Doctoral School, Óbuda University, Hungary
- <u>orcid.org/0000-0002-2540-9027</u>

Author 11

- James Leak, Ph.D.
- School of Computing, Engineering and the Built Environment, Edinburgh Napier University, Edinburgh, United Kingdom

Author 12

- Daniel Barreto, M.Sc., Ph.D, DIC.
- School of Computing, Engineering and the Built Environment, Edinburgh Napier University, Edinburgh, United Kingdom
- <u>orcid.org/0000-0003-4790-3250</u>

#### Full contact details of the corresponding author.

- Daniel Barreto, M.Sc., Ph.D, DIC.
- School of Computing, Engineering and the Built Environment, Edinburgh Napier University, Merchiston Campus, Edinburgh, United Kingdom, EH105DT
- <u>orcid.org/0000-0003-4790-3250</u>
- E-mail: d.barreto@napier.ac.uk

#### Abstract

Estimation of hydraulic conductivity in soils is challenging. The primary aim of this study is to demonstrate that such predictions may be improved if grading curves are appropriately quantified and described, as well as by including density-related values in such relationships. Various saturated hydraulic conductivity models were tested with the assumption that predictions would improve if different grading curve statistics are used. A unimodal database was elaborated using old and new data. Three types of permeability models were examined. One using the traditional

variables consisting of the product of harmonic mean  $d_h$  or  $d_{10}$  and void ratio, the hydraulic radius; as well as additional density information. The second using the grading entropy coordinate pair  $S_{0,} \Delta S$  or the similar pair  $d_{10}$ ,  $C_{U}$ , expressing the mean grain size on logarithmic scale along with the spread of the grain size distribution and containing similar information on pore size distribution (POSD) by duality. When these were combined in the third type, including also relative density for coarse materials, the fit was the best, verifying the hypothesis that the full pore size range may be the missing pore geometry information of the Taylor's equation (hence predictions are better if grading curve parameters consider the entire distribution of particle sizes). The parameters identified for the various data series were dependent on the data themselves as found from early times in literature. The similarity of grading entropy coordinate pairs and the pair  $d_{10}$ ,  $C_{U}$ , as well as  $d_h$  and  $d_{10}$ , was analysed by simulations and by using the same measured data.

#### Keywords chosen from the ICE Publishing list

Granular materials; Permeability & pore-related properties; Statistical analysis

#### List of notations

Α	is the relative base entropy
В	is the normalised entropy increments
$C_U$	is the coefficient of uniformity (= $d_{60}/d_{10}$ )
$C_i$	are model parameters
Cs	is the skew
Ск	is the kurtosis
CV	coefficient of variation (Standard deviation/expected value)
<b>d</b> <sub>h</sub>	is the harmonic mean diameter
<b>d</b> <sub>10</sub>	is the diameter of which 10% of the particles are finer
<b>d</b> 50	is the diameter of which 50% of the particles are finer
<b>d</b> 60	is the diameter of which 60% of the particles are finer
е	is the void ratio
<b>e</b> <sub>max</sub>	is the maximum void ratio
<b>e</b> <sub>min</sub>	is the minimum void ratio
k	is the saturated hydraulic conductivity in [cm/s]
<i>v,</i> N	is the fraction number
$R_D$	is the relative density
r <sub>m</sub>	is the hydraulic radius
$ ho_{ m v}$	is the pore volume on unit pore surface
$ ho_{ m s}$	is the grain density

- $S_s$  is the surface area of voids
- S<sub>0</sub> is the base entropy
- $\Delta S$  is the entropy increment
- $S_{sA}$  is the specific surface area per volume [1/m]
- $S_{sm}$  is the specific surface area per mass [m<sup>2</sup>/g]
- SD standard deviation
- PSD is the particle size distribution
- POSD is the pore size distribution
- GSD is the grain size distribution by dry mass
- V is the total volume
- $V_{\nu}$  is the volume of voids
- $V_{\rm s}$  is the volume of solid
- $x_i$  is the relative frequency of fraction *i*

#### 1 1. Introduction

The estimation of hydraulic permeability in coarse-grained is challenging. Consequently, several relationships have been proposed (e.g. Hasen, 1893; Kozeny, 1927; Taylor, 1948; Carrier, 2003; Ren & Santamarina, 2018). It is also relatively well accepted that permeability is affected by particle morphology and mineralogy (e.g. Li, et al 2023). Chen, et al (2019) have further considered the effect of grading on permeability at the pore scale. However the focus of the present study is that some existing studies have considered the effect of void ratio and grain size distribution on the estimation of hydraulic conductivity.

9

10 With regards to grain size distributions, it is common for existing relationship to use parameters 11 such as  $d_{10}$ ,  $d_{50}$  and  $c_u$  (= $d_{60}/d_{10}$ ) which do not fully quantify/describe the entire grading curve. It 12 is hypothesized that better estimations of hydraulic conductivity can be made if parameters that 13 characterise the entire grading curve and alternative measures of density are also used for such 14 estimations. To demonstrate such hypotheses, we perform statistical analyses on a combined 15 granular database of hydraulic conductivity experiments, and we have re-evaluated results 16 obtained by other researchers. The combined database has been complemented by new and 17 extensive experiments by the authors covering a very wide range of grading curves for coarse-18 grained soils. Using the full database, the variables of both the classical theory and the grading 19 entropy theory were applied to develop empirical relationships between grading curves and 20 hydraulic conductivity.

21

22 The structure of the paper is as follows. Hereafter, the grain size distribution (GSD), pore size 23 distribution (POSD) and density variables for saturated hydraulic conductivity models of granular 24 materials are summarized. Then the Taylor's permeability model-the foundation of all 25 subsequent models—is presented, highlighting its open question regarding the description of 26 pore geometry and the assumption of this research. Next, we present the methods of data 27 processing, parametric model definition, parameter identification, and model discrimination. 28 Moreover, we detail the results concerning the established database, elaborated models, along 29 with the results of the model discrimination. Finally, we discuss the elaborated model equations

```
30 and analyse the similarities among various grading curve variables (S_0 - \Delta S and d_{10} - C_U,
```

31 moreover,  $d_h$ -  $d_{10}$ ).

32

### 33 1.1 Grain size distribution curve and statistics

The measured grading curve represents a finite, discrete distribution with *N* uniform statistical cells, based on *N* sieve data (Figure 1). Using a logarithmically uniform cell system representing the size fractions (Table 1, Appendix 1), some additional statistical variables can be defined beyond the traditional quantiles like  $d_{60}$ ,  $d_{50}$ ,  $d_{10}$  and other derived quantities such as the coefficient of uniformity  $C_U$  as follows.

39

40

#### 41 Table 1. Fraction *i* in terms of diameter *d* and *D* (dimensionless diameter variable)

Fraction number <i>i</i>	1	23	24
Limits in terms of d	1 d <sub>0</sub> to 2 d <sub>0</sub>	$2^{22} d_0$ to $2^{23} d_0$	$2^{23} d_0$ to $2^{24} d_0$
$D \text{ or } S_{0i}[-]$	1	23	24

42

43 1.1.1. Harmonic mean diameter and related variables

44 The harmonic mean diameter (*d<sub>h</sub>*) from all measured GSD data is computed as follows:

45

$$46 \qquad d_h = \frac{1}{\sum_{i=1}^N \frac{x_i}{d_i}}$$

47 1.

48

49 where *d<sub>i</sub>* is an arbitrary diameter value selected from fraction ("sieve") *i*. This value can be chosen

50 in various ways, however the choice of diameter has a negligible effect on the results.

51

52 The mean pore volume is defined as (Imre *et al.*, 2014):

53 
$$\rho_v = \frac{V_v}{S_s}$$

54 2.

56 where  $V_v$  is the volume of voids and  $S_s$  is the specific surface.  $\rho_v$  may also be expressed using

58 
$$\rho_{\nu} = \frac{V - V_s}{6V_s \sum_{i=1}^N \frac{x_i}{d_i}} = \frac{1}{6} \frac{e}{\sum_{i=1}^N \frac{x_i}{d_i}} = \frac{e}{6} d_h,$$

59 3.

60 where e is the void ratio. It can be noted that the value of the mean pore volume is equal to the

- 61 hydraulic radius  $r_m$  (Taylor, 1948), containing the product of the void ratio and the harmonic mean
- 62 diameter.

63

64 The specific surface area per volume of the soil is defined as:

65

66 
$$S_{sA} = \frac{6}{(1+e)} \sum_{i=1}^{N} \frac{x_i}{d_i} = \frac{6}{(1+e)d_h},$$

67

4.

68

69 The specific surface area per mass of the soil is defined as:

70 
$$S_{sm} = \frac{6}{\rho_s} \sum_{i=1}^{N} \frac{x_i}{d_i} = \frac{6}{\rho_s d_h}$$

71

5.

72

- 73 1.1.2. The grading entropy coordinates
- 74 In Figure 1, the GSD is represented, where the sieve fractions, with sieve hole diameters doubling
- at each step, create a uniform cell system. The four grading entropy coordinates, derived from all
- 76 measured GSD data, are calculated as follows (Lorincz, 1986, Singh, 2014).
- 77

$$78 \qquad S_0 = \sum x_i \, S_{0i}$$

6.

79

80

$$81 \qquad A = \frac{S_0 - S_{0min}}{S_{0max} - S_{0min}}$$

82 7. 83  $\Delta S = \frac{-1}{\ln\left(2\right)} \sum_{i=1}^{N} x_i \ln x_i$ 84 85 8. 86  $B = \frac{\Delta S}{\ln N}$ 87 88 9. 89 90 where  $S_{0i} = i$  is the *i*-th fraction entropy (see Table 1), N is the number of fractions including the 91 smallest and largest diameter non-zero fractions. 92 93 The  $d_0$  in Table 1 is limited by the smallest diameter which may approximately be equal to the 94 diameter of the SiO₄ tetrahedron (~2.68E-8 m). In this work, d₀=3.05175E-08 m is used. It can be 95 noted that the relation between diameter limits and the  $S_{0i}$  is not unique. 96 97 By specifying the arbitrary smallest (*i*-th) and the arbitrary largest ((i+N-1)-th) non-zero fractions, 98 infinite many grading curves can be defined. It can be shown that for every fixed value of A, the 99 subgraph area of the related GSD-s is the same, and there is a unique, optimal grading curve 100 with maximum B and finite fractal distribution. Since this optimal grading curve has no inflexion 101 point, it is a kind of mean grading curve. It follows that the fractal grading curve series depending 102 on A can be used to elaborate "mean" relationships of the various grading curve statistics (Imre 103 et al., 2022). 104 105 1.2 Density type permeability model variables 106 The density variables employed in the saturated hydraulic conductivity models of granular 107 materials are summarized hereafter. The most popular density variables are the void ratio (e), the 108 porosity (n), dry density ( $\rho_d$ ), the solid volume ratio (s) or its inverse, the specific volume (v). Their 109 basic relations are given below:

110	
111	$n = 1 - \frac{1}{1+e} = \frac{e}{1+e}$
112	10.
113	
114	$e = \frac{1-s}{s}$
115	11.
116	
117	$s = \frac{1}{1+e} = \frac{1}{v}$
118	12.
119	
120	$ \rho_d = s \rho_s $
121	13.
122	
123	The most informative parameter is the relative density ( $I_D$ or $R_d$ ), which is dependent on three
124	variables: the void ratio e and the minimum and maximum dry densities in terms of emax and emin:
125	
126	$I_D = \frac{e_{\max} - e}{e_{\max} - e_{\min}}$
127	14.
128	
129	Notably, (Kabai, 1974) observed that the ratio $e_{min} / e_{max}$ remains approximately constant for most
130	sands but begins to decrease as the soil contains more silt, see some values in (Imre et al., 2011).
131	Furthermore, the $e_{max}$ of fractal grain size distributions has a minimum at A=2/3 by observation
132	which is also a boundary defining stable and instable packings, (e.g. Lorincz, 1986; Imre et al.,
133	2019). In practical terms this highlights that grading entropy parameters may be as or more useful
134	than common parameters such as $C_u$ and $d_{10}$ to define the suitability of granular filters and the
135	stability of fills and embankments.
136	
137	

138 1.3 The Taylor's equation; aim and structure of the paper 139 In Taylor's derivation, the saturated permeability relation is derived from Poiseuille's law of 140 hydraulics, considering soil pores as a group of tubes. The Taylor permeability equation (Taylor, 141 1947), reads: 142  $k = \left(\frac{V_v}{S_s}\right)^2 \frac{\gamma_w}{\mu} \frac{e}{(1+e)} C = r_m^2 \frac{\gamma_w}{\mu} \frac{e}{(1+e)} C,$ 143 144 15. 145 146 where  $\gamma_{w}$  is permeant's unit weight,  $\mu$  is the dynamic viscosity of the permeant. The  $r_{m} = ed_{n}/6$  is 147 the hydraulic radius or the mean pore size in the case of spherical grains, e/(1+e) is the 148 porosity, and the free parameter C depends on additional pore geometry characteristics. It 149 follows that a good permeability model may contain the product of the third power of void ratio 150 and the second power of the harmonic mean diameter. 151 152 In the present study it was assumed that the pore geometry can be characterized by the four 153 grading entropy coordinates (i.e. Eqs 5 - 8). These are precise grading curve statistics, based 154 on all data measured during sieving. Hence they can enhance the accuracy of the soil 155 permeability models. 156 157 It is well-known that the  $S_{o}$ ,  $\Delta S$  and their normalised forms A and B, are related to a kind of 158 mean logarithmic grain diameter, to the spread of the distribution (similar to  $C_{U}$ ) and to the 159 internal structure and stability information. 160 161 In the present study, the pairs  $S_0 - \Delta S$  and  $d_{10} - C_U$  were incorporated into various permeability 162 models. The parameters of the so defined models depending on the underlying data, (Taylor, 163 1948), were identified using a new database containing relatively unimodal grain size 164 distributions, ranging from silt to gravel sizes. 165 166 2. Methods

#### 167 2.1 Databases

168	The databases used in the present study correspond to both existing and new hydraulic
169	conductivity experiments. Existing databases were chosen with the aim of considering grading
170	effects including particle sizes ranging from silts to gravels. Furthermore, it is considered
171	important to make comparisons that involve identical testing conditions and repeatability. In that
172	regard all tests and series included consider constant head tests with identical testing conditions
173	and many of them with repeated measurements that add reliability to our databases.
174	
175	Series 1 to 4 are based on the research of the Central Organisation for Flood Protection, Hungary,
176	collecting different soils from 10 pits along various dikes. The series were created by mixing soils,
177	ranging from silt to gravel, with four fixed, different $d_{10}$ ranges in the silt fraction between 0.006 to
178	0.016mm. As increasing amounts of coarse materials were added, the mixtures became
179	progressively bimodal, with $C_U$ ranging from 2 to 530. Falling head tests were repeated three
180	times on 74 soil mixtures (Nagy, 2011, 2012); the saturated hydraulic conductivity ranged from
181	6E-6 to 5E-3 cm/s.
182	
183	Series 5 (coarse sand and fine gravel) was based on the database by Feng, et al (2019). The
184	soils had a $d_{10}$ range of 0.72 to 5.82 mm, $C_U$ ranged from 1.9 to 6.9, saturated hydraulic
185	conductivity (constant head test) ranged from 0.378 to 50.107 cm/s. At least half of the samples
186	were significantly bimodal.
187	
188	Series 6 to 8 are from Pap and Mahler (2018) and Nagy 92010, 2011). Series 6 comprises various
189	soils and measuring techniques extending for finer soils. The $d_{10}$ ranged of 0.004 to 0.01 mm, $C_U$
190	ranged from 3 to 84, saturated hydraulic conductivity (constant head test) ranged from 1E-7 to
191	1E-6 cm/s. Series 7 and 8 are part of Nagy's data (Series 1 to 4). Hence partly overlapping Series
192	1 to 4.
193	
194	In the present research, some new measurements were conducted by the authors on 2-fraction
195	soils with four fractions: 0.25-0.5 mm (medium sand), 0.5-1 mm and 1-2 mm (coarse sand), and

196  $\,$  2-4 mm (fine gravel). These comprised Series 9 and 10 featuring 15 (one repeat) and 45 (3

197 repeats) results on 15 identical compositions, differing only in density. The  $d_{10}$  range was of 0.28 198 to 1.4 mm, Cu ranged from 1.6 to 2.2, saturated hydraulic conductivity (constant head test) ranged 199 from 0.079 to 2.2 cm/s. 200 201 In the data processing phase, the Weibull fitting (Guida et al., 2016; Casini et al., 2017) was 202 applied, to provide the ordinates of the GSD in the cell system (Table 1) and some completion 203 of the measured data for fines, if it was needed. Then - besides the traditional quantile 204 parameters and derived grading curve parameters, including  $d_{10}$ ,  $d_{30}$ ,  $d_{50}$ ,  $d_{60}$  and the uniformity 205 coefficient  $C_U$  - the four grading entropy coordinates and central moments (based on parameter 206 D in Table 1) were computed. Bimodal grading curves were excluded based on the normalised 207 grading entropy coordinate values (see Appendix 1). Where the fine content was not precisely 208 measured in series 1 to 4, the PSD was extrapolated below d=2E-3 mm down to dmin=6.1E-05 209 mm (which generally did not influence the value of  $d_{10}$ ). 210 211 2.2 Permeability modelling 212 2.2.1 Some existing models 213 The simplest, single-linear models contain only  $d_{10}$ , like the model in (Hasen, 1893): 214 215  $k = 1.3C_H d_{10}^2$ 216 16 217 218 where the parameter  $C_H$  is Hazen's empirical coefficient and  $d_{10}$  is the characteristic particle 219 diameter. 220 221 Lumped/composite parameters are commonly used because (i) the hydraulic radius component 222 of Taylor's model (Equation 15) is the product of a diameter value and the void ratio, (ii) density 223 is an important additional variable. An example is the Chapuis's equation (Chapuis, 2004): 224  $e^3$  1<sup>0.7825</sup> Г

225 
$$k = 2.4622 \left| d_{10}^2 \frac{c}{1+e} \right|$$

226 17. 227 228 In the context of multi-variable models with parameters identifiable through multiple linear 229 regression, certain variable pairs can be highlighted (Carman, 1937, 1939). For example, 230 (Kozeny, 1927) gives the following formula by using a value for  $d_{10}$  less than 1.0 mm: 231  $k = 1.2 C u^{0.735} d_{10}^{0.89} \frac{e^3}{l+e}$ 232 233 18. 234 235 Carrier (2003) proposes a similar equation using  $d_h$ . Instead of using  $d_{10}$  and  $C_U$  the grading 236 entropy coordinates pairs (A, B) and ( $S_0$ ,  $\Delta S$ ) along with void ratio were used by Feng et al. (2017) 237 and Imre et al. (2021). 238 239 2.2.2 The parametric models used in the model discrimination study 240 The following parametric models were included in the model discrimination study. 241 242 A single-variable model with two unknown parameters given by the expression: 243  $k=C_1\,p^{C_2}$ 244 245 19. 246 247 where parameters  $C_1$  and  $C_2$  depend on the unit of the variables p and k. The p is either a diameter 248 value (e.g., d10, d30, d50, d60 and dn) or a lumped/composite variable. The latter is the product of 249 some diameter value or a harmonic mean - based variable, the void ratio and the porosity, expressed, for example, as  $d_{10}^3 e^3/(1+e)$ . 250 251 252 The parametric form of the model by Ren & Santamarina (2018): 253 254  $k = C \cdot S_{sA}^{-2} e^{C_2}$ 

255	20.
256	
257	Note that for comparison with Equation 19, $C_1 = C S_{sA^2}$ .
258	
259	Multivariable models with three or four unknown parameters were also used:
260	
261	$k = \exp C_3 \Delta S^{C_1} S_0^{C_2}$
262	21.
263	
264	$k = \exp C_4 \Delta S^{c_1} S_0^{c_2} p^{c_3}$
265	22.
266	
267	The base entropy S <sub>0</sub> and the entropy increment $\Delta S$ were exchanged with $d_{10}$ and $C_U$ in some
268	cases (and with A and B, see section 4).
269	
270	2.2.3 Model fitting, discrimination and validation methods
271	The inverse problem was linear for most of the considered conductivity models when using the
272	logarithmic form of Equation 21 (or 22), e.g.:
273	
274	$\ln k = C_3 + C_1 \ln \Delta S + C_2 \ln S_0  \text{and}$
275	$\ln k = C_4 + C_1 \ln \Delta S + C_2 \ln S_0 + C_3 \ln p$
276	
277	23.
278	
279	The (multi-)linear model fitting was based on the weak solution of the Gauss Normal Equations
280	of the formulated inverse problem. Subsequently, the standard deviation and coefficient of
281	variation were estimated (Press et al., 2007). The model discrimination was based on either the
282	minima of the normalised merit function called fitting error $F$ or on the $R^2$ value (defined as one
283	minus the ratio of the residual variance to the total variance of the dependent variable, quantifying
284	the fraction of data variance explained by the model). The results of the model discrimination

study are further analysed in Appendix 2, which explores the dependence of model parameters

- 286 on the data used for identification and evaluates model accuracy both on the training data and
- withheld data.
- 288
- 289 **3. Results**
- 290 3.1 The database
- 291 3.1.1 Grading curve statistics

The results are shown in Figures 2 to 4, and Tables 1 and 2, as well as Appendix 1. The Weibull fitting provided the ordinates of the GSD in the cell system (Table 1) to compute the various GSD statistics. Highly bimodal samples were left out on the basis of the GSD statistics (see Appendix 1). According to the results (Imre *et al.*, 2021), the entropy coordinates changed significantly if the fines were considered by extending the grading curves up to the possible smallest grain sizes which were not measured. The precise value of the fines in the grading curve measurement was essential for the normalized entropy coordinates.

- 299
- Table 2 contains the range and mean values of the  $d_{10}$  and  $C_U$  for the selected samples, Table 3 contains the range and mean values of the non-normalised grading entropy coordinates for the selected samples. It can be seen that the mean of  $S_0$  increases for Series 1 to 5, the mean of  $\Delta S$ decreases for Series 1 to 5 with series number and there is a gap between Series 4 and 5. The mean of the selected grading curves of the various series is shown in Figure 2(b). The grading

306 curves of the selected and all samples of Series 1 to 4 are shown in Figure 3. The grading entropy 307 coordinates of the selected samples of the old series, the planned samples (to address the gap) 308 and of the new series are shown in Figure 4(a), in the non-normalised grading entropy diagram. 309 The three groups of grading curves of the new Series 9 and 10 (with identical composition) are 310 shown in Figure 4(b).

- 311
- 312 Table 2. The statistical features of selected data.

*d*10 [mm]

 $C_U[-]$ 

Series	mean	min	max	mean	min	max	
1	0.0055	0.0042	0.0065	27	19	36	
2	0.0117	0.0076	0.0154	30	22	38	
3	0.0195	0.0089	0.0805	14	2	14	
4	0.0391	0.0101	0.0990	13	4	36	
5	2.4196	0.7200	5.8200	4.08	2	7	
9 – 10*	0.7000	0.2800	1.5900	1.9313	1.59	2.15	

313 \*new data, entire series

314

315 Table 3. Some statistics of the non-normalised entropy parameters of selected mixtures

	mean S <sub>0</sub>	min S₀	$\max S_0$	mean $\Delta S$	min $\Delta S$	$max\Delta S$
1	12.8	11.0	14.4	3.2	1.9	3.8
2	14.2	12.0	16.1	3.2	2.4	3.7
3	14.6	11.7	19.1	2.9	1.1	3.5
4	15.2	11.4	18.2	2.6	2.2	3.5
5	17.5	16.1	18.6	1.6	0.6	2.2
9 – 10*	16.5	15.3	17.8	0.9	0.8	1.00

316 \*new data, entire series

317

318 3.1.2 Saturated water hydraulic conductivity

319 In Figure 5, the k is shown in terms of the single (diameter or lumped) curve variables. Each  $d_i$ 

320 correlated positively; the best was the  $d_{10}$ . However, the lumped variables like  $d_{10}d_{10}e^{3}/(1+e)$  with

321 extra porosity term showed correlation improvement.

322

In Figure 6, the *k* is shown in terms of  $C_U$  and in terms of  $S_0$  and  $\Delta S$ . Nagy's research gave separate equation of type A/( $C_U$  +B)+C  $d_{10}^2$  for series 1 to 4, with parameters A, B and C, predicting decrease with  $C_U$  and increases with  $d_{10}$ .

326

327 In Figures 6(a), (b), semi-linear correlation trends of hydraulic conductivity in terms of  $C_U$  are 328 shown at the various fixed  $d_{10}$  range for the unimodal samples of Series 1 to 4, and an evidence

329 of suffosion. There is a basically increasing trend with the series number (related to increasing 330  $d_{10}$  ranges) and decreasing with increasing  $C_{U_1}$  in accordance to (Nagy, 2011). A similar trend is 331 shown in Figure 6(c) and (d) in terms of the entropy coordinates: k decreases with increasing  $\Delta S$ , 332 like with  $C_U$ , and increases with increasing  $S_0$ , similarly to  $d_{10}$ , but with a less significant 333 correlation. This will be discussed in section 4.3. 334 335 In Figure 7, the k is shown in terms of simple, single variable  $S_{SA}$ , the relative density and the 336 lumped Santamarina's variable, moreover the e is shown in terms of sample number 1 to 15, for 337 the new 2-fraction coarse mixtures. 338 339 The regression is not acceptable in terms of single variables without density term only. The k-340 relative density graphs exhibit significant separation between loose and dense samples and 341 among grain sizes as follows. In coarsest group 1 k ranges from 0.05 to 0.09 cm/s for dense 342 and from 0.22 to 0.48 cm/s for loose samples. In group 2 k ranges from 0.03 to 0.06 cm/s for 343 samples and from 0.13 to 0.27 cm/s for loose samples. In finest group 3 k ranges from 0.007 to 344 0.012 cm/s for dense and from 0.05 to 0.14 cm/s for loose samples. The great difference can 345 tentatively be explained by a different – possibly honeycomb – structure for the loose samples. 346 347 The Taylor equation simplifies assuming that parameter C is constant as follows: 348  $\frac{k_1}{k_2} = \frac{e_1^2}{e_2^2}$ 349 350 24. 351 352 Since identical samples were tested at different densities, the fit to Equation 24 was used to 353 indicate the different structure for the denser samples and the looser samples. 354 355 In Figure 7(d), e values are depicted, with  $e_{min}$  and  $e_{max}$  derived from the literature. The  $e_{max}$  was 356 measured by (Lorincz, 1986) on samples with identical composition, while emin was estimated 357 based on data from (Kabai, 1974, Imre et al., 2011).

358	
359	3.2 Model discrimination results
360	The results are shown in Tables 4 to 6, and are presented separately for the old part, the new
361	part and the entire unimodal database (Figure 2(a)).
362	
363	3.2.1.1 Old part of database (joint series 1 to 5)
364	The results are shown in Table 4. The following is the fitting quality in accuracy increasing order:
365	1. Single variable using diameter - type variables (e.g., $d_{10}$ ).
366	2. Grading entropy parameter pair only.
367	3. Lumped single variable with porosity.
368	4. Grading entropy parameter pair combined with void ratio (density information).
369	5. Grading entropy parameter pair combined with lumped variables, which provided the best
370	accuracy.
371	
372	The pair $S_0$ - $\Delta S$ was found interchangeable with the pair $d_{10}$ - $C_U$ . The latter gave slightly worse
373	values for $R^2$ as for the grading entropy parameters only and a similar value as when using $d_{10}$
374	alone. This indicates that the pair $S_0$ - $\Delta S$ was better for representing the data than the pair $d_{10}$ -
375	C <sub>U</sub> .
376	

#### Table 4. Model discrimination based on the old database, using Series 1-5 jointly..

variable <i>p</i>	R <sup>2</sup> (multiple linear model,	R <sup>2</sup> (single-linear	
	entropy parameters and <i>p</i> )	model with <i>p</i> )	
$d_{10} \cdot d_{30} \cdot d_{60} \cdot e^3 / (1+e)$	0.963	0.949	
$d_{10}^2 \cdot e^3/(1+e)$	0.968	0.946	
1	0.934*		
$d_{10}$		0.9117	
$d_{30}$		0.8231	
$d_{60}$		0.716	
е	0.953	0.131	

378	* $C_U$ , $d_{10}$ gave $R^2$ =0.9074
379	
380	3.2.1.2 Elaborated single-variable models
381	
382	The elaborated equations for the single variables are shown in Equations 25 to 28. For the
383	predictor variable $d_{10}$ , the following equation resulted ( $R^2=0.9117$ ):
384	
385	$k = 0.878 \ d_{10}^{2.0213}$
386	25.
387	
388	This is the Hazen equation (Hazen, 1893) with fitted model parameters for this database.
389	The equation obtained with $R^2$ =0.823 employing as a predictor variable $d_{30}$ reads
390	
391	$k = 2.265 d_{30}^{2.5571}$
392	26.
393	
394	The equation with $R^2$ =0.716 using as a predictor variable $d_{60}$ is:
395	
396	$k = 6.047 d_{60}^{2.6393}$
397	27.
398	
399	In terms of $d_{10}^2 e^3/(1+e)$ , the regression analysis gives for k with $R^2 = 0.946$ the following:
400	
401	$k = 5.868 \left[ d_{10}^2 \frac{e^3}{1+e} \right]^{1.0322}$
402	28.
403	
404	This is the Chapuis's equation (Chapuis, 2004) adapted to the new soil data set (the original
405	equation fits the data with $R^2$ =0.2025).

407 3.2.1.3 Elaborated multi-variable models

408	Concerning the multi-variable Equations 21, 22; results are shown in Tables 5 and 6 and in
409	Equations 29 to 32. The parameters were determined in the equivalent, natural logarithm form
410	Equation 22. The exponents of the entropy increment $\Delta S$ and the base entropy $S_0$ were the
411	identified parameters $C_1$ , $C_2$ , and the coefficient in Equation 21 was equal to $exp(C_3)$ .

412

Table 5 shows the parameters of the 3-parameter entropy variable equation fitted on individual Series 1 to 5. The parameters depended on the position of series in the entropy diagram (see Appendix 2), the difference was more significant than the linear error of the parameter identification. The absolute value of the exponent of  $\Delta S$  was between 0.45 and 6.41, and the value of the exponent of  $S_0$  was between 2.8 and 32.9. The exponent of  $\Delta S$  decreased, while the exponent of  $S_0$  increased as soil became coarser.

419

420 Table 5 Results of fit of the 3-parameter Equation 21, using data from Series 1 to 5 and joint

421 Series 1 to 4, parameter estimates and fitting errors (selection of S<sub>0</sub>, as shown in Appendix 1).

422

Series	5	1	2	3	4	14
C <sub>1</sub>	-0.45	-3.80	-1.63	-1.23	-0.93	-6.41
C <sub>2</sub>	32.87	7.11	-4.58	7.77	2.76	4.69
<i>C</i> <sub>3</sub>	-92.46	-23.68	3.88	-27.24	-13.82	-14.34
$SD(C_1)$	0.59	1.15	0.44	3.44	1.13	0.92
$SD(C_2)$	4.96	1.81	0.68	8.82	2.09	1.58
$SD(C_3)$	14.39	4.94	1.40	18.80	4.45	3.97
CV( <i>C</i> <sub>1</sub> )	-1.32	-0.30	-0.27	-2.80	-1.21	-0.14
CV( <i>C</i> <sub>2</sub> )	0.15	0.25	-0.15	1.13	0.76	0.34
$CV(C_3)$	-0.16	-0.21	0.36	-0.69	-0.32	-0.28
Fitting Error [-]	0.07	2.7E-4	2E-2	2.6E-2	4.8E-3	2E-02

423

Table 6 shows the estimated parameters of the various 4-parameter entropy variable equations identified using joint Series 1 to 5. The absolute value of the exponent of  $\Delta S$  was between 2.4 and 6.2, and the value of the exponent of  $S_0$  was between 2.6 and 22.2. The value of the coefficient *C* varied between exp(-59.4) to exp(-5.7), small numbers occurred being in the same interval as for the 3-parameter case.

429

430 The sign of the exponent of  $S_0$  was generally positive, and the sign of the exponent of  $\Delta S$  was 431 generally negative. The coefficient of variation was smaller for the "global" equation (using joint 432 Series 1-5) than for the series separately.

433

434 Table 6 Results of the fit of the 4-parameter equations, estimated parameters, coefficients of

435 variation and R<sup>2</sup>

p	<i>d</i> <sub>10</sub> <i>d</i> <sub>10</sub> <i>e</i> <sup>3</sup> /(1+ <i>e</i> )	<i>d</i> <sub>10</sub> <sup>3</sup> <i>e</i> <sup>3</sup> /(1+ <i>e</i> )	$d_{10}d_{30}d_{60}e^{3}/(1+e)$	е	entropy parameters only
<i>C</i> <sub>1</sub>	-2.4	-3.0	-3.3	-3.2	-6.2
<b>C</b> <sub>2</sub>	8.8	8.3	2.6	22.3	17.5
C₃	0.6	0.3	0.4	5.1	-46.6
$C_4$	-22.3	-21.1	-5.7	-59.4	
$CV(C_1)$	-0.3	-0.2	-0.2	-0.2	-0.1
CV( <i>C</i> <sub>2</sub> )	0.2	0.2	1.0	0.1	0.1
CV( <i>C</i> <sub>3</sub> )	0.1	0.1	0.1	0.2	0.1
CV( <i>C</i> <sub>4</sub> )	-0.2	-0.2	-1.2	-0.1	2
$R^2$	0.968	0.965	0.963	0.953	0.934

436

The fitting error was smaller if individual Series 1 and 4 were considered. If Series 2, 3 and 5, or
Series 1-4 or 1-5 were used jointly in derivations, the magnitude of the fitting eeror was up to two
orders of magnitude larger.

440

441 Some equations obtained using Series 1 to 5 jointly are:

443	$k = 7.67\text{E-}21  \Delta S^{-6.21}  \text{S}_0^{-17.51}$	
444	29.	
445		
446	$k = 2.38\text{E}-26\Delta S^{-3.24}S_0^{-22.28}e^{5.15}$	
447	30.	
448		
449	$k = 0.003375  \Delta S^{-3.32}  S_0^{2.64}  [d_{10}d_{30}d_{60}  e^3/(1+e)]^{0.43}$	
450	31.	
451		
452	$k = 2.40\text{E-10}\Delta S^{-2.4}\text{S}_0^{-8.8}[d_{10}^2e^3/(1+e)]^{0.6}$	
453	32.	
454		
455	3.2.2. New data	
456	Using new data for two-fraction mixtures consisting of medium- to	coarse-grained sand and fine
457	gravel, with identical composition but different densities, the model	fitting yielded an R <sup>2</sup> value less
458	than 0.2 when density was not considered as an extra variab	le and was greater than 0.8
459	incorporating the pair of grading entropy coordinates and the rela	ative density parameter (Table
460	7).	
461		
462	Table 7, New data (small $C_U$ ), model discrimination,	
	Independent variables (predictors)	R <sup>2</sup>
	Entropy parameters and relative density	0.8746
	Entropy parameters and void ratio	0.7811
	Entropy parameters	0.1700
463		
464	3.2.3 New and old data together	

465 Being included old and new data (Series 1-5, 9-10), using the Ren and Santamaria model on 150

466 samples, the identified with  $R^2 = 0.846$  exponent of the void ratio was 8.6, i.e.:

468	$k \sim \frac{e^{8.6}}{S_{SA}^2}$
469	33.
470	
471	The fitting of the multiple linear equation using the grading entropy parameters and the Ren-
472	Santamarina's variable was successful, achieving $R^2$ of 0.924. The equation with the estimated
473	parameters reads:
474	
475	$k = 1.729 \cdot 10^{-19} \Delta S^{1.005} \cdot S_0^{-17.5} \cdot [e^{8.6} / S_{sA}^2]^{0.53}$
476	34.
477	
478	4. Discussion
479	4.1 The analysis of the results
480	Various analyses were performed on the results. First, the effect of the training data on the
481	identified parameters and on the model accuracy were considered. The case in which training
482	data were selected is considered in detail in Appendix 2 (Figures A2-1 and 2, Table A2-1). The
483	identified parameters of Equation 21 – depending on the two grading entropy variables - were
484	represented in 1-dimensional form by fixing the one variable. The functions did not intersect
485	each-other if the "hulls" of the entropy coordinates of the training data series were disjunct. The
486	multivariable Equation 21 was more precise if the training data and the tested data were similar.
487	The single-variable Equation 19 (the simple $d_{10}$ - model) was more precise if the training data
488	set was larger than the tested data set. The model discrimination result of the original Series 1
489	to 4 (with bimodal samples) aligned with the foregoing result, however, there was a notable
490	disparity in the $R^2$ values where gap-graded soil with possible suffusion were included.
491	
492	4.2 Some results with normalised grading entropy coordinates and with level lines
493	
494	The definition of N - the number of fractions including the smallest and largest non-zero fractions
495	- is not the same in the literature, for example in (Feng et al., 2019), the arbitrary smallest and
496	largest fractions can be zero fractions. The so computed coordinates are not differing from the

497 non-normalised coordinates due to the functional relationships defined by Equations 6 to 9. The498 two approaches are equivalent; only numerical differences may occur.

499

500 This similarity is illustrated in Figure 8 where the permeability zones and k-level lines are 501 presented in the non-normalised and normalised entropy diagrams. The results are also similar 502 to the earlier data of (Feng et al., 2019).

503

Feng *et al.*, 2019 used normalized entropy coordinates *A* and *B* for Equations 21 and 22, in combination with the void ratio. For Series 5, models employing the independent variable combinations A - B, and A - B - e showed  $R^2$  values of 0.90 and 0.96, respectively. In contrast, for the joint unselected Series 1-2, the  $R^2$  values were 0.23 and 0.27 (Imre *et al.*, 2021). These results support the present model discrimination study.

509

However, in the internal stability rule of the grading entropy concept, based on the entropy coordinate *A*, the sharp definition of *N* is needed. In future research, it would be interesting to combine the non-normalised grading entropy coordinates with the normalised entropy coordinate *A*, computed using the sharp definition of *N*. Some early results are presented on the effect of A in (Imre *et al.*, 2020).

515

#### 516 **4.3 The grading curve statistics**

517 The pair  $S_0 - \Delta S$  was found interchangeable with pairs  $d_{10} - C_U$  (or A - B, using the wider definition 518 of *N*). To explain this, simulations of mean relations using fractal or mean grading curves (see 519 section 1) and experimental data were considered in Figures 9 and 10, respectively.

520

According to Figure 9, the theoretical mean relations for  $\Delta S - C_U$  determined using fractal grading curves with *N*=5, 7 and 20 are non-unique (different branch is related to *A*< or *A* > 2/3) while the theoretical mean relations for *A* -  $d_{10}$  determined using fractal grading curves with *N*= 7 is unique.

525 In Figure 9(a), the measured, unselected data are within, the gap-graded data are outside the 526 band bounded by the theoretical mean  $\Delta S - C_U$  relation. Similarly, the experimental relation of

527	selected data for $\Delta S$ - $C_U$ seems to have a regression along the area bounded by the theoretical
528	band of the mean relation (Figure 10(a)). The regression is stronger for $S_0 - d_{10}$ along the
529	theoretical, unique, mean relation (Figure 10(b)). The theoretical, mean relations may explain that
530	the regression $C_U$ - $\Delta S$ gives slightly smaller $R^2$ than the regression $d_{10}$ - $S_0$ .
531	
532	Concerning other regressions to measured $S_0$ - $d_i$ data (Table 8, Figure 10(c)), $R^2$ is larger for $S_0$
533	- $d_{60}$ than for $S_0$ - $d_{10}$ since $d_{60}$ is closer to the mean abstract diameter value, which is the meaning
534	of S <sub>0</sub> . Concerning the experimental relation for Series 2 and 5, the regressions $d_{10}$ - $d_h$ and $d_{10}$ - $r_m$

are linear is semi-log plot. The  $d_h$  was slightly larger than  $d_{10}$  for gravel and that  $d_h$  was smaller

536 than  $d_{10}$  for fine sand. Further research is suggested on this matter.

537

538 Table 8. Multiple linear regression results for the independent variable combinations of  $S_0$  and 539 selected  $d_i$ .

Variable	$R^2$	Equations
$d_{10}$	0.7672	$\ln S_0 = 0.0587 \ln d_{10} + 2.8628$
$d_{30}$	0.8494	$\ln S_0 = 0.0777 \ln d_{30} + 2.8138$
$d_{60}$	0.8363	$\ln S_0 = 0.0886 \ln d_{60} + 2.7553$

540

#### 541 **5. Summary and conclusions**

542

#### 543 **5.1 Model discrimination**

544 The parametric saturated hydraulic conductivity models examined here were three types. The 545 first model set was based on single, classical variables like the harmonic mean  $(d_h)$  or  $d_{10}$ , the 546 void ratio e, porosity e/(1+e) or a lumped variable of these. The second model set was based on 547 variable pairs (the non-normalised grading entropy coordinate pair  $S_0$  -  $\Delta S$  or the pair  $d_{10}$  -  $C_U$ ). 548 The third model set was based on the combination of variables of the first model set and on a 549 variable pair of the second model sets. 550 551 A unimodal database was started to be built for this purpose re-evaluating some previous 552 databases and providing some new data for granular materials ranging from silt to gravel. The

553	bimodal samples of the old databases were left out since for these mixtures the permeability
554	test was not precise due to suffusion. The identification of the parameters of the suggested
555	models was made by multiple linear regression based on various subsets of the new database.
556	The $R^2$ was generally significant, but the result was the best when thy model sets 1 and 2 were
557	combined. The difference among the model variants was small for Series 5 with small $C_{U}$ .
558	
559	All identified parameters depended on the range of grading entropy coordinates of the data
560	used for parameter identification, as well as implicitly on grain shapes and other factors.
561	The successfully tested models were as follows:
562	single-variable models, using one lumped variable consisting of some squared diameter
563	variables and at least the second power of void ratio, or more complicated forms, like
564	$d_{10} \cdot d_{30} \cdot d_{60} \cdot e^3/(1+e)$ being related to the hydraulic radius and the porosity terms of
565	Taylor's equation;
566	• .multi-variable models, with a variable pair $S_0 - \Delta S$ or pair $d_{10} - C_U$ (alone or being
567	completed by either a density terms or one of the previous lumped variables), expressing
568	the missing pore geometry information of Taylor's equation.
569 570	5.2 Taylor equation
571	The Taylor equation contains the porosity, squared hydraulic radius (mean pore volume), and
572	the constant that expresses the pore geometry. This fact may explain why most $k$ - models
573	contain the third product of the void ratio and the second pore a diameter value (the best is the
574	harmonic mean diameter based on the fraction cell system and all measured data).
575	
576	The grading entropy theory (Lorincz, 1986) offers a coplementary statistical system of
577	quantifying the GSD, using all data measured in the sieving test. The model discrimination
578	results supported the hypothesis that the non-normalised grading entropy parameters may give
579	information on the geometry of GSD (mean abstract diameter and spread of the distribution)
580	and by duality on the geometry of POSD, which is needed for the Taylor equation.
581	

#### 582 **5.3 Future research**

583	In future research, in the multivariable models, the non-normalised grading entropy coordinates
584	are planned to be completed by the normalised entropy coordinate A, computed using the sharp
585	definition of N which may link some additional packing information.
586	
587	The dependencies of the parameters on the data used for model fitting are planned to be
588	quantitatively determined in future research. To achieve this, the database will be completed
589	and parallel tests with varying grain shapes, e.g., laboratory experiments and numerical
590	simulations using the discrete element method, are planned to be conducted. More research is
591	needed on the present database and on the suggested models families.
592	
593	The relative density giving the best result for sands as density variable, depending on three
594	parameters (the void ratio e, the emax, emin being the void ratio at minimum and maximum dry
595	densities) can be a relevant parameter of the future saturated hydraulic conductivity of sands.
596	Note that our data analysis has considered the use of void ratio both as an individual and
597	lumped/composite grain-size permeability relationships. It can be determined from two tests
598	only, based on the research of (Kabai, 1974,) using that the ratio $e_{max}/e_{min}$ is about constant.
599 600	Acknowledgements
601	The discussions with Professor Nagy and Professor Paul Vardanega are greatly acknowledged.
602	The help of former students Levente Répássy, Dang Thi Quynh Huong, and Lizeth Lamas Lopez
603	is acknowledged. M. Datcheva acknowledges the partial support by Grant No BG05M2OP001-
604	1.001-0003-C01, financed by the Science and Education for Smart Growth Operational Program
605	(2014-2020) and co-financed by the European Union through the European Structural and
606	Investment funds. D. Barreto acknowledges the support provided by the Royal Academy of
607	Engineering Leverhulme Trust Fellowship 2023 (LTRF2223-19-134) that enabled him to focus on
608	research work.
609	

### 610 Contributions

611 Emoke Imre. Conceptualisation. Data curation. Formal analysis. Funding acquisition.612 Methodology. Writing. Review and editing.

- 613 Zsombor Illés. Conceptualisation. Data curation. Investigation. Writing
- 614 Francesca Casini. Data curation. Investigation. Validation
- 615 Giulia Guida. Data curation. Investigation. Validation
- 616 Shuyin Feng. Data curation. Validation. Writing
- 617 Maria Datcheva. Conceptualisation. Data curation. Funding acquisition. Methodology.
- 618 Writing. Review and editing.
- 619 Wiebke Baille. Data curation. Investigation. Validation
- 620 Ágnes Bálint. Conceptualisation. Methodology. Writing. Review and editing.
- 621 Delphin Kabey Mwinken. Investigation. Validation
- 622 János Lorincz. Conceptualisation. Methodology. Writing
- 523 James Leak. Data curation. Investigation. Writing. Review and editing.
- 624 Daniel Barreto. Conceptualisation. Data curation. Funding acquisition. Writing. Review and 625 editing.
- 626

## 627628 References

- 629 Casini F, Guida G, Bartoli M, Viggiani GMB (2017) Grading evolution of an artificial granular
- 630 material from medium to high stress under one-dimensional compression. Rivista Italiana di
- 631 Geotecnica 51(4): 69–80, <u>https://doi.org/DOI:10.19199/2017.4.0557-1405.69</u>
- 632 Carman PC (1937) Fluid flow through granular beds. Chemical Engineering Research and
- 633 Design 15: S32–S48, <u>https://doi.org/10.1016/S0263-8762(97)80003-2</u>
- 634 Carman PC (1939) Permeability of saturated sands, soils and clays. The Journal of Agricultural
- 635 Science 29(2): 262–273, <u>https://doi.org/10.1017/S0021859600051789</u>
- 636 Carrier WD (2003) Goodbye, Hazen; Hello, Kozeny-Carman. Journal of Geotechnical and
- 637 Geoenvironmental Engineering 129(11): 1054–1056, <u>https://doi.org/10.1061/(ASCE)1090-</u>
- 638 <u>0241(2003)129:11(1054)</u>
- 639 Chapuis RP (2004) Predicting the saturated hydraulic conductivity of sand and gravel using
- 640 effective diameter and void ratio. Can Geotech J 41(5): 787–795, <u>https://doi.org/10.1139/t04-</u>
- 641 <u>022</u>
- 642 Chen, R.-P, Liu, P., Liu, X.-M, Wang, P.-F. & Kang, X. (2019) Pore-scale model for estimating
- 643 the bimodal soil-water characteristic curve and hydraulic conductivity of compacted soils
- with different initial densities. Engineering Geology, 260, 105199,
- Feng S (2017) Assessing the permeability of pavement construction materials by using grading
  entropy theory. MSc thesis, University of Bristol, Bristol, UK

- 647 Feng S, Vardanega PJ, Ibraim E, Widyatmoko I, Ojum C (2019) Permeability assessment of
- 648 some granular mixtures. Géotechnique 69(7): 646–654, <u>https://doi.org/10.1680/jgeot.17.T.039</u>
- 649 Guida G, Bartoli M, Casini F, Viggiani GMB (2016) Weibull Distribution to Describe Grading
- 650 Evolution of Materials with Crushable Grains. Procedia Engineering 158:75–80,
- 651 https://doi.org/10.1016/j.proeng.2016.08.408
- Hazen A (1893) Some physical properties of sand and gravels. Massachusetts State Board of
- Health, Wright & Potter Printing, Boston, MA, USA, pp.
- Imre E, Fityus S, Keszeyné E, Schanz T (2011) A Comment on the Ratio of the Maximum and
- 655 Minimum Dry Density for Sands. Geotechnical Engineering Journal of the SEAGS &
- 656 AGSSEA 42(4):77–82.
- 657 Imre E, Lorincz J, Hazay M, Juhász M, Rajkai K, Schanz T, Lins Y, Singh VP, Hortobágyi Zs
- 658 (2014) Sand mixture density in: of UNSAT2014. pp. 691–697.
- Imre E, Lorincz J, Barreto D, Trang PQ, Csonka I, Kaczvinszki-Szabó V, Telekes G. (2019)
- 660 Preliminary study on the relationship between dry density of sands and the grading entropy
- parameters. XVII ECSMGE. Reykjavík, Iceland : 1–6 of September 2019 pp. 996-1002.
  Paper: 167797.
- 663 Imre E, Balint A, Barreto D, Khaliunaa A, Boldbaatar T, Dang T, Guadalupe L, Illés Z (2020) The
- 664 Saturated Hydraulic Conductivity of 2-Fraction Granular Soils and the Internal Stability, In:
- 665 Hosam, E.A.F. Bayoumi Hamuda.11th International Annual Conference on Sustainable
- 666 Environmental Protection & Waste Management Responsibility, ICEEE 2020: Proceedings
- 667 Book. Budapest, Magyarország: Óbudai Egyetem, pp. 267-274.
- Imre E, Bálint Á, Nagy L, Lorincz J and Illés Zs (2021) Examination of saturated hydraulic
- 669 conductivity using grading curve functions, in Proceedings of 6th International Conference on
- 670 Geotechnical and Geophysical Site Characterisation, Budapest, Hungary, pp. 1–12.
- 671 Imre E, Hortobágyi Zs, Illés Zs, Nagy L, Talata I, Barreto D, Fityus S, Singh VP (2022) Statistical
- 672 parameters and grading curves. In: Rahman R, Jaksa J (eds) Proceedings of the 20th
- 673 International Conference on Soil Mechanics and Geotechnical Engineering. Australian
- 674 Geomechanics Society, Sydney Australia, pp 713–718

- 675 Imre E, Firgi T, Baille W, Datcheva M, Barreto D, Feng S, Singh V (2023) Soil parameters in
- 676 terms of entropy coordinates. E3S Web of Conf. (Vol. 382, p. 25003). UNSAT 2023,
- 677 https://doi.org/10.1051/e3sconf/202338225003
- 678 Kabai I (1974) The effect of grading on the compatibility of coarse-grained soils. Periodica
- 679 Polytechnica Civil Engineering 18(4):255-275.
- 680 Kozeny J (1927) Über kapillare Leitung des Wassers im Boden. Akademie der Wissenschaften,
- 681 Wien, pp 271–306
- 682 Li, S.-L., He, R.-J and Kang, X. (2023). Permeability of polymer-modified kaolinite and fly ash-
- 683 kaolinite mixtures. Géotechnique Letters, 13:4, 211-217
- 684 Lorincz J (1986) Grading entropy of soils Doctoral Thesis. Technical Sciences, TU of Budapest, 685 Hungary
- 686 Lorincz J, Imre E, Fityus S, Trang P, Tarnai T, Talata I, Singh V (2015) The Grading Entropy-
- 687 based Criteria for Structural Stability of Granular Materials and Filters. Entropy 17(5): 2781-
- 688 2811, https://doi.org/10.3390/e17052781
- 689 Nagy L (2011) Permeability of well graded soils. Per Pol Civil Eng 55(2): 199-204,
- 690 https://doi.org/10.3311/pp.ci.2011-2.12
- 691 Nagy L (2012) Characterization of piping with grading entropy on the Surány example. Per Pol
- 692 Civil Eng 56(1):107-113, https://doi.org/10.3311/pp.ci.2012-1.12
- 693 Pap M, Mahler A (2018) Comparison of Different Empirical Correlations to Estimate
- 694 Permeability Coefficient of Quaternary Danube Soils. Period Polytech Civil Eng 63(1): 25-2,
- 695 https://doi.org/10.3311/PPci.13108
- 696 Press WH, Teukolsky SA, Wetterling WT, Flannery BP (2007) Numerical recipes in C: the art of
- 697 scientific computing. Second Edition, Cambridge University Press, Cambridge, UK; New 698
- York, pp. 1-994.
- 699 Ren XW, Santamarina JC (2018) The hydraulic conductivity of sediments: A pore size
- 700 perspective, Engineering Geology, 233: 48–54, <u>https://doi.org/10.1016/j.enggeo.2017.11.022</u>
- 701 Singh VP. Entropy theory in hydraulic engineering: an introduction (2014). American Society of
- 702 Civil Engineers, p.656.
- 703 Taylor DW (1948) Fundamentals of soil mechanics. John Wiley & Sons, Inc., New York, USA,
- 704 pp. 1–700.

706	
707	Figure captions
708 709	Figure 1. (a, b) Grain size distribution and density functions of a sand. Legend: in terms of
710	diameter d (dashed line); in terms of abstract diameter D (solid line), see Table 1.
711	
712	Figure 2. Data processing of old and new samples (a). Weibull fit, with completion for fines (series
713	2, sample 13, bimodal). (b) Mean, selected, unimodal-grading curves for series 1 to 9.
714	
715	Figure 3. Sample selection for series 1-4. (a) Selected unimodal samples. (b) All samples.
716	
717	Figure 4. Data processing results of old and new samples. (a) Selected, new and planned samples
718	in the non-normalised grading entropy diagram. (b) Series 9 (= 10), grading curves of new, 2-
719	fraction mixtures, three groups, serial numbers (sample id-s) 1 to 15.
720	
721	Figure 5. The saturated hydraulic conductivity in terms of a single variable. (a) to (c) $k$ in terms of
722	$d_{10}$ , $d_{30}$ , $d_{60}$ , respectively (each $d_i$ correlates positively, and the best is $d_{10}$ ). (d) k in terms of lumped-
723	variable of the Chapuis model (significant improvement in correlation).
724	
725	Figure 6. The saturated hydraulic conductivity in terms of elements of pairs $d_{10}$ - $C_U$ or $\Delta S$ - $S_0$ .
726	(a) The k in terms of $C_{U}$ , Series 1 to 4, selected samples, and (b) Series 2, all samples (gap-
727	graded, non-selected soils showed suffusion). (c) and (d) The k in terms of $\Delta S$ and $S_0$ .
728	
729	Figure 7. Newly measured 2-fraction mixtures data. (a) to (c): Saturated hydraulic conductivity in
730	terms of $S_{sA}$ ; relative density; Ren and Santamarina variable; resp. (d) the void ratio with
731	approximate values at the maximum and minimum dry density. Legend: circles - loose samples,
732	squires – dense samples.
733 734	Figure 8 The zones of saturated permeability $k$ (a) Approximate level lines in non-normalised
735	entropy diagram (Imre et al., 2021). (b) Series 5 in the normalised entropy diagram (Feng et al.
736	2019) (c) The same as (a) in the normalised diagram.

738	Figure 9. Mean relations of fractal soils, various <i>N</i> values. (a) $C_U - \Delta S$ with measured,
739	unselected data for Series 3, the unimodal samples are within the band of mean relation, (b)
740	d <sub>10</sub> - A.
741	
742	Figure 10. (a) and (b): The experimental, relations $C_U$ - $\Delta S$ and $d_{10}$ - $S_0$ on selected data. (c) The
743	experimental relations of $d_{10}$ - $d_h$ and $d_{10}$ - $r_m$ , Series 2 and 5 data.
744	
745	Figure A2-1. The simplified $k$ – models related to Equation 21 with parameters identified from
746	various training series. (a) with respect to $\varDelta S$ and (b) with respect to $S_0$
747	
748	Figure A2-2. Goodness-of-fit for models using various datasets. (a) results considering Eq. 21.
749	(b) results considering Eq. 19. (c) results considering Eq. 21 and a larger dataset. (d) Model
750	performance in terms of d <sub>10</sub>
751	
752	

## 754 Appendix 1 Some notes to the fraction system, and to the use of the abstract diameter

An abstract fraction system is given in terms of *d*<sub>0</sub> being limited by the smallest diameter, some

related information is given in Table A1-1 The soil types related to the suggested *d*<sub>0</sub> and base

entropy values are shown in Table A1-2 in two different ways.

Table A1 -1. Diameter sizes

order of magnitude	size in m	2 <sup>n</sup> , exponent <i>n</i>	fraction serial number
	1.53E-08	-26	0
SiO <sub>4</sub> tetrahedron	3.05E-08	-25	1
a few microns	3.91E-06	-18	8*
1 mm sieve	1.00E-03	-10	16
gravel	6.40E-02	-4	22
km (~4 km)	4.19E+03	12	38

<sup>759 \*</sup>Range of comminuting limit of small particles by compression (Kendall, 1978)

760

761

Table A1-2. The soil fractions in terms of abstract diameter D

name	gravel	sand	silt
<i>d</i> [mm]	32-2	2-0.0625	0.065 - 0.001955
$S_{0i}$ or $D[-]$	20 - 17	16– 12	11 - 7
S <sub>0i</sub> or D [-]*	21 - 18	17 - 13	12 - 8

<sup>&</sup>lt;sup>\*</sup>alternative, upper values (Tables 4 to 6 are based on the values in row 2).

763

Using the fact, that the normalized grading entropy parameters A and B have unique, monotonic

765 mean relationship with the skewness and kurtosis of (of abstract diameter) variable D, the

various soil series were tabulated in terms of these. Extreme values indicated bi-unimodal, near

767 gap-graded soils which were left out from the unimodal database (Table A1 - 3).

768

Table A1-3. Selecting unimodal grading curves on the basis of skew  $C_S$  and kurtosis  $C_K$  of D

and the normalised grading entropy coordinates, on the example of Series 1. Extreme values

(deviating most from the mean) were bi-modal, near gap-graded soils (indicated in bold).

	CS	А	Ск+3	В
1*	-1.08	0.68	5.05	1.00
2	-0.58	0.56	3.36	1.16
3	-0.45	0.56	3.05	1.21
4	-0.41	0.58	2.74	*1.28
5	-0.20	0.59	2.30	1.28
6	-0.11	0.61	1.99	1.26
7	0.16	0.64	0.83	1.32
8	-1.29	0.60	4.67	1.03
9	-1.46	0.66	4.99	0.86
10*	0.07	0.64	1.08	1.29
11*	0.06	0.67	0.89	1.25
12*	-1.86	0.57	6.57	0.90
13*	-1.52	0.57	5.53	0.97
mean	-0.67	0.61	3.31	1.14

773

## 774775 Appendix 2: Discussion of the models

The following questions were investigated to prove the reliability of the new modelsl, using

various training and testing datasets, in a prelimary manner.

778

779 Question 1. How does the simulated *k* with Eq 21 at various training datasets compre in terms

780 of the entropy variables?

781 In Eq 21, the k is a function of  $\Delta S$  and S<sub>0</sub>. The parameters identified by the various training data

subsets are different, as shown in Tables 5, 6. The question how the identified coefficients of

Figure 783 Equation 21 may vary in terms of various training data subsets was examined such that  $\Delta S - k$ 

functions and  $S_0 - k$  functions were defined by using fixed  $S_0$  and  $\Delta S$ , resp., (being equal to the

785 mean value given in Table 3). In Figure A2-1(a) and (b), generally the *k* decreases with  $\Delta S$  and

786 increases with S<sub>0</sub> but differently for the various subsets. The Series 1 appears disjoint in (also

787 in the entropy diagram, Figure 2(a)).

788	Question 2. How does the goodness of k simulated with Eq 21 and Eq 19 compare at various
789	training set on general data of Series 2?
790	The prediction accuracy of Equation 21 and 19 was tested using the whole, unselected Series
791	2. The results are shown in Figure A2-2 (a) and (b). For Eq 21 (with only entropy variables),
792	the prediction was better for smaller than from larger training data set. For Eq 19 (with only $d_{10}$ ),
793	the reverse was true. In other words, the finding was different for Equation 21 and for 19.
794	
795	Question 3. How does the goodness of $k$ simulated with Eq 21 compare at various training set
796	on selected data of Series 1 to 4? The accuracy of Equation 21 (prediction with only on entropy
797	parameters) on selected series 1 to 4 was tested. The prediction was better for smaller than
798	from larger training data set set (Figure A2-2 (c)), similarly to the previous case.
799	
800	Question 4. How does the k simulated with Eq 21 and Eq 19 compare in terms of $d_{10}$ ?
801	The $S_0$ - $d_{10}$ relation determined here (see Table 8) was used to change variable $S_0$ into $d_{10}$ , and
802	the value of DS was fixed at various values. It was found in Figure A2- 2(d) that the tested
803	models were basically similar in terms of $d_{10}$ . It is important to note that the entropy variable
804	based equation does not work for DS =0, but is working for DS >0.5.
805	
806	Question 5. How does the model rank compare on general data (interpolation case)?
807	Four models were used, $p$ , $S_0 - \Delta S$ , $S_0 - \Delta S - e$ , and $S_0 - \Delta S - p$ where $p$ was the Ren-Santamarina's
808	variable with exponent 8. The results showed the same model discrimination results as for the
809	selected series, according to result in Table A2-1, for various models, considering the complete
810	data, the $R^2$ variation was similar. Series 2 showed the worse result, possibly due to the
811	inclusion of the gap-graded mixtures showing suffusion during the permeability test.
812	
813	Question 6. How is the goodness of fit of various models for extrapolation?
814	Seven experiments of Series 9 were used to validate the elaborated relationships presented in
815	this study. The results in Table A2-2 were characterized by the mean squared difference of the
816	measured and computed values, called variance here. The most sophisticated model-versions
817	Eq 22 were not working (with entropy parameters and <b>p</b> ), the single variable models Eq 19 and

- 818 the only entropy parameter models Eq 21 were better. The d<sub>10</sub> equation without any other
- 819 variables also provided good results.
- 820
- 821 Table A2-1. The R<sup>2</sup> in case of various model variables, non-selected samples

series	test #	р	$S_0$ , $\Delta S$	$S_0$ , $\Delta S$ , e	S <sub>0</sub> ,ΔS, p
1	13	0.0613	0.7077	0.7093	0.7119
2	18	0.1837	0.2424	0.2519	0.3088*
3	30	0.0107	0.6117	0.595	0.5963
4	12	0.4362	0.622	0.7086	0.7593
5	30	0.8905	0.83	0.8917	0.9362

822 Note: The variable p was Ren & Santamarina's (2018) variable with exponent 8

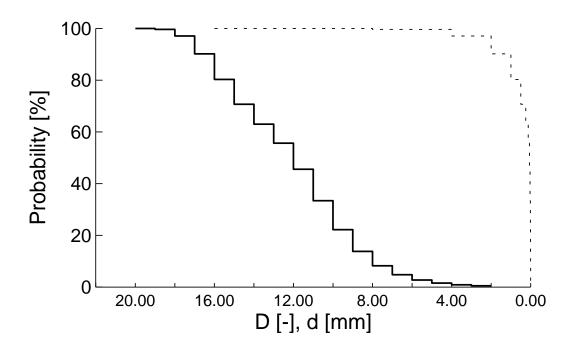
823

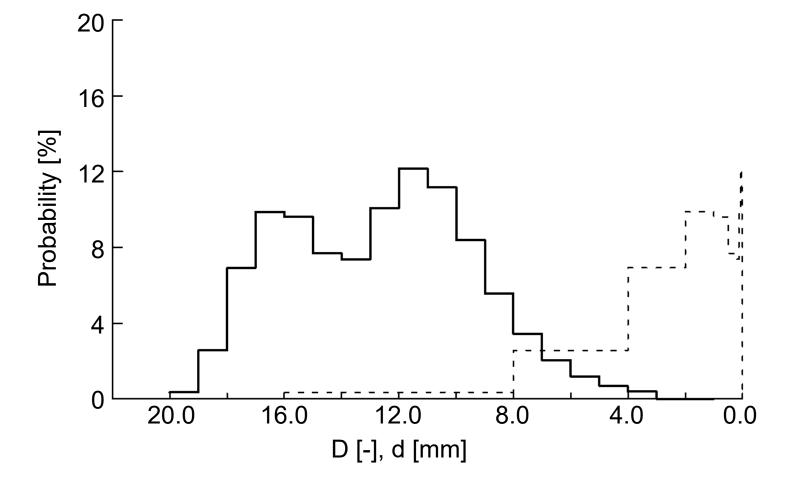
Table A2-2. The variance of extrapolation error, training data set 1..5, tested data from series 9.

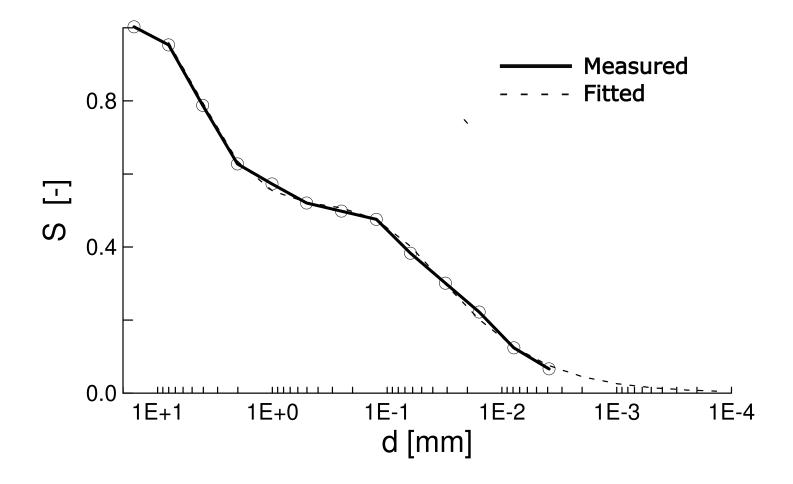
	Eq 21 º	Eq 22+	Eq 22+	Eq 19 *
р	-	d <sub>10</sub> <sup>2</sup> e <sup>3</sup> / (1+e)	d <sub>10</sub> * d <sub>30</sub> * d <sub>60</sub> * e <sup>3</sup> /(1+e)	d <sub>10</sub> <sup>2</sup>
error	1.1	57.7	28.9	0.4

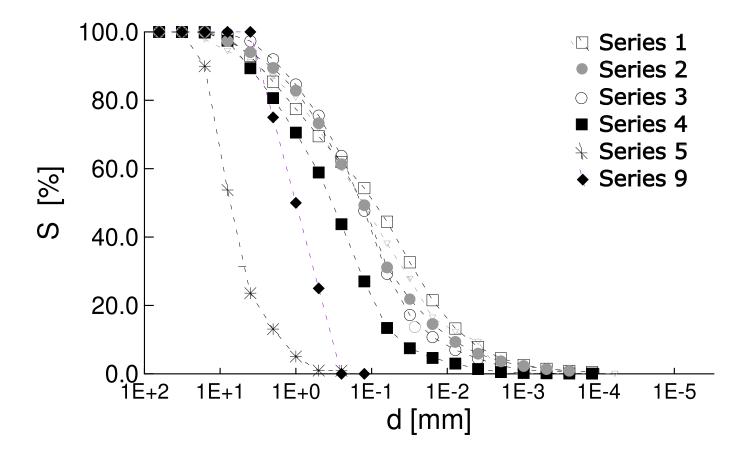
825 <sup>o</sup> only entropy coordinates, \* classical variables only, + with entropy coordinates

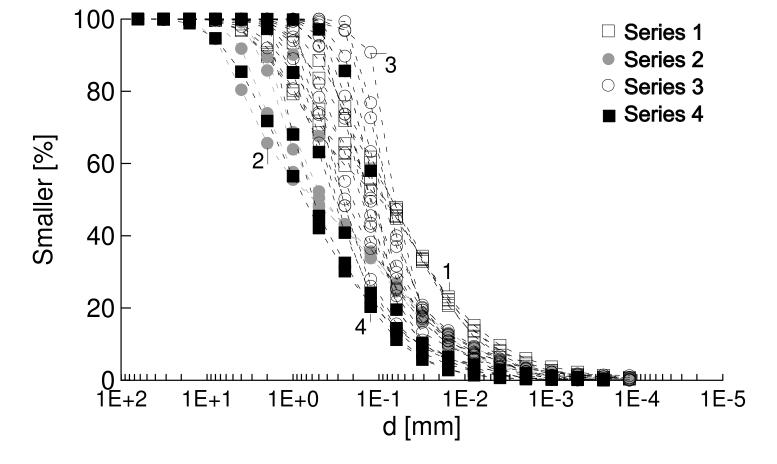
826

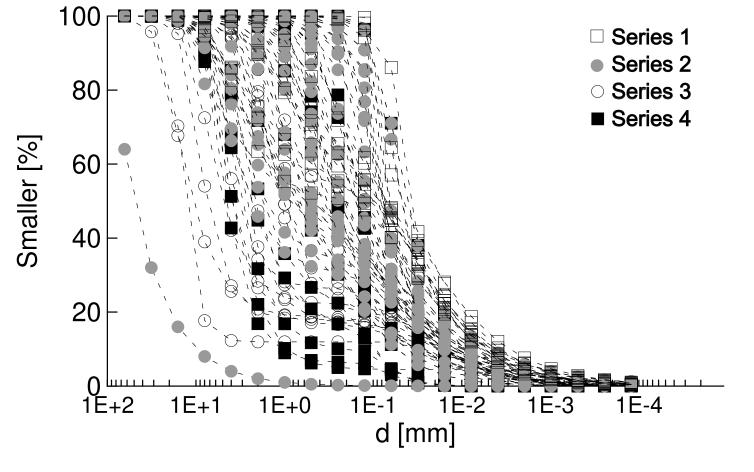


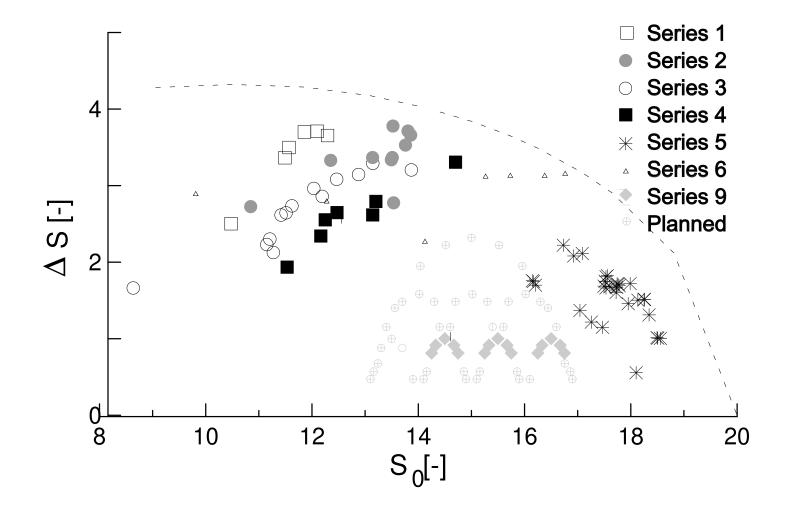


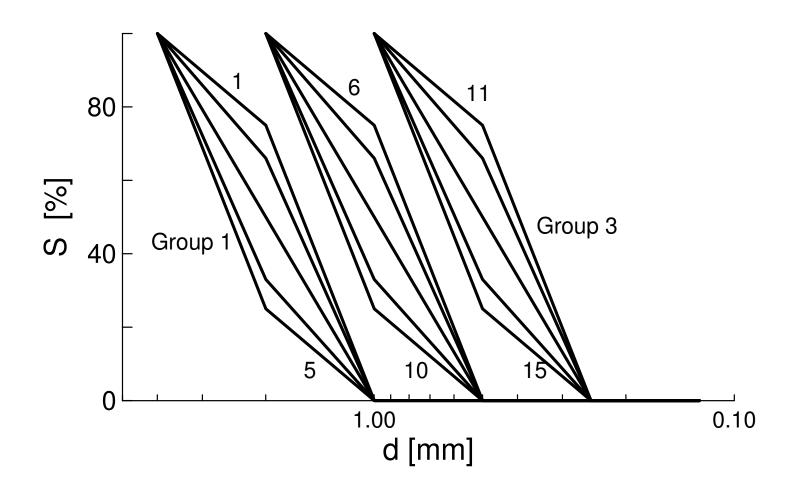


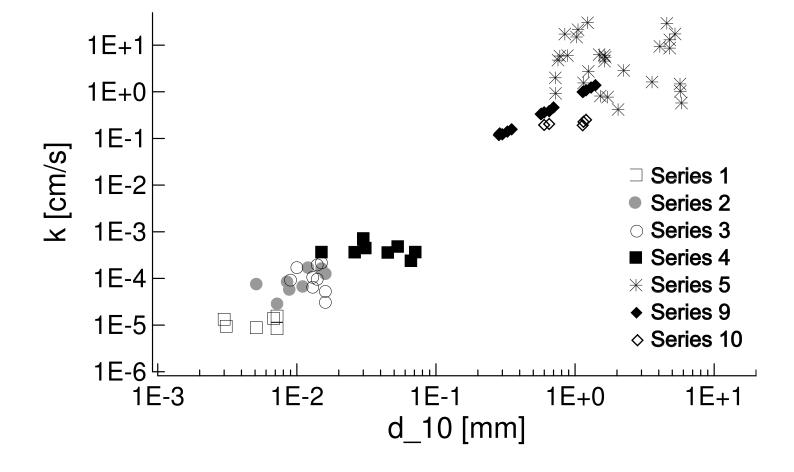


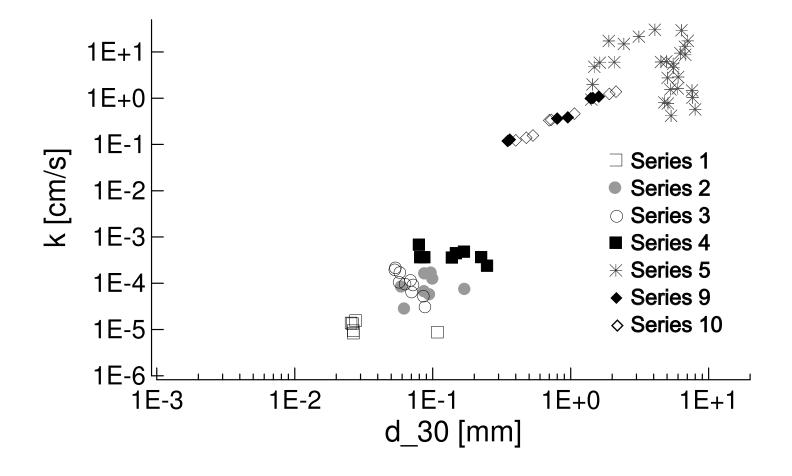


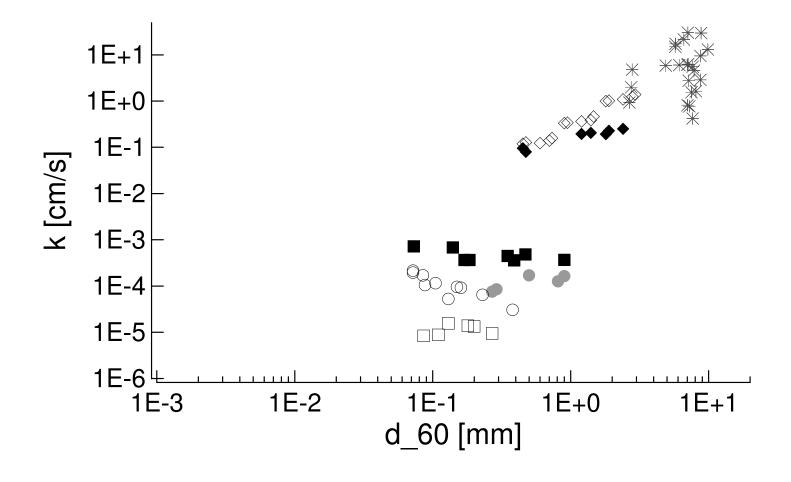


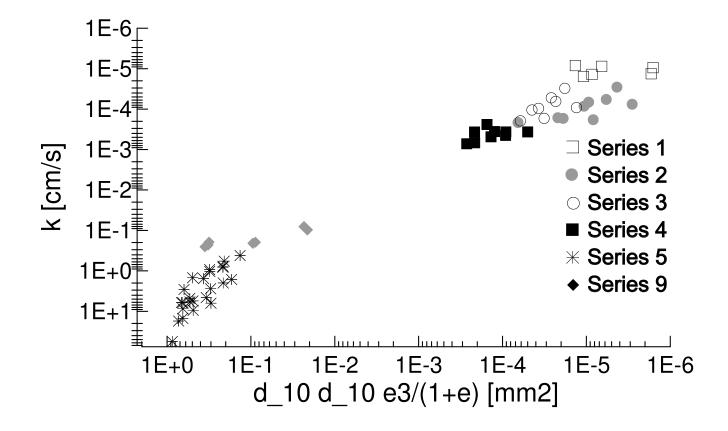


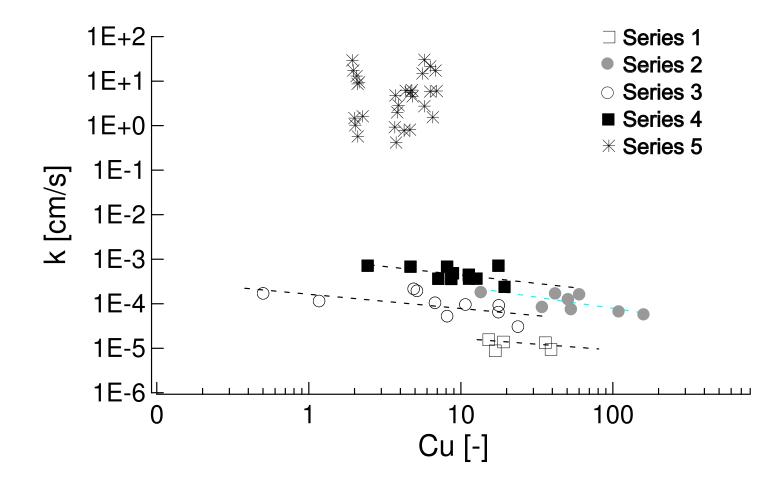


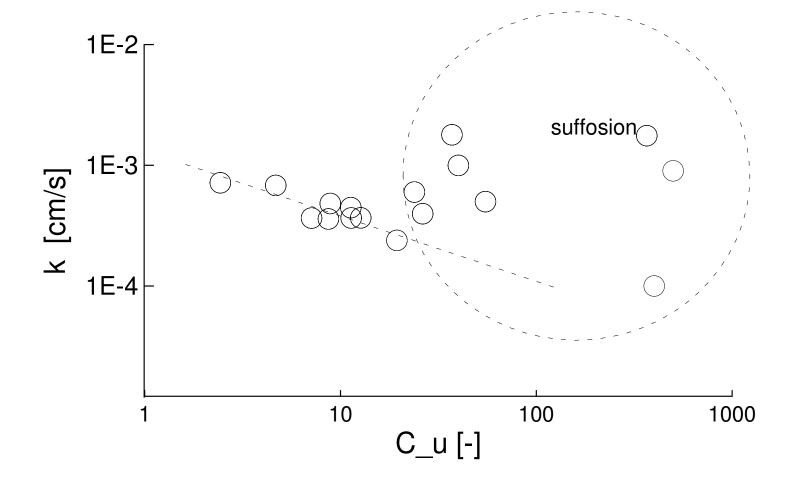


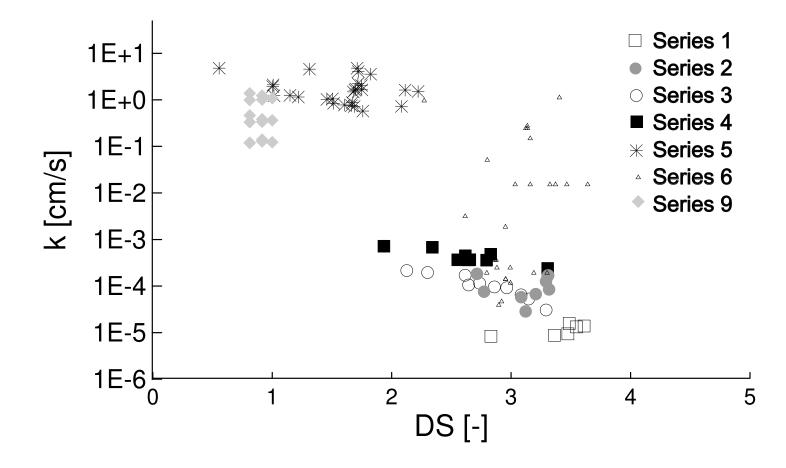


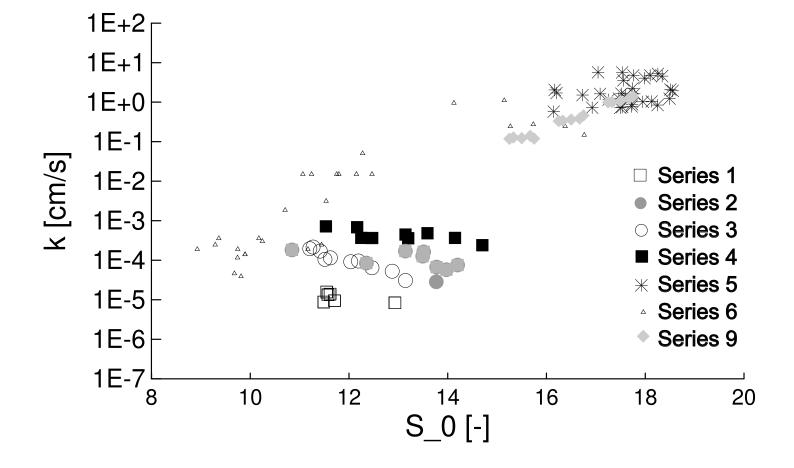


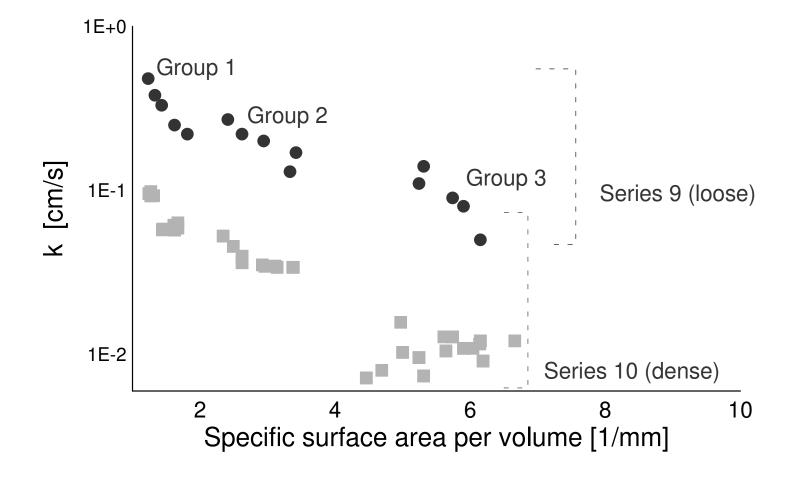


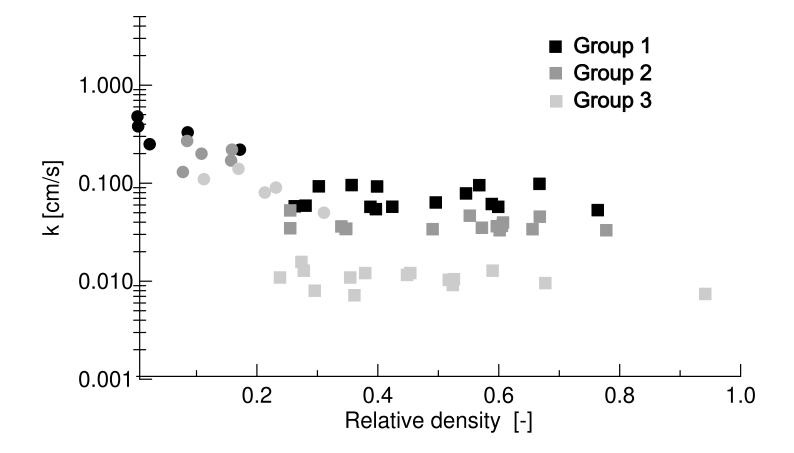


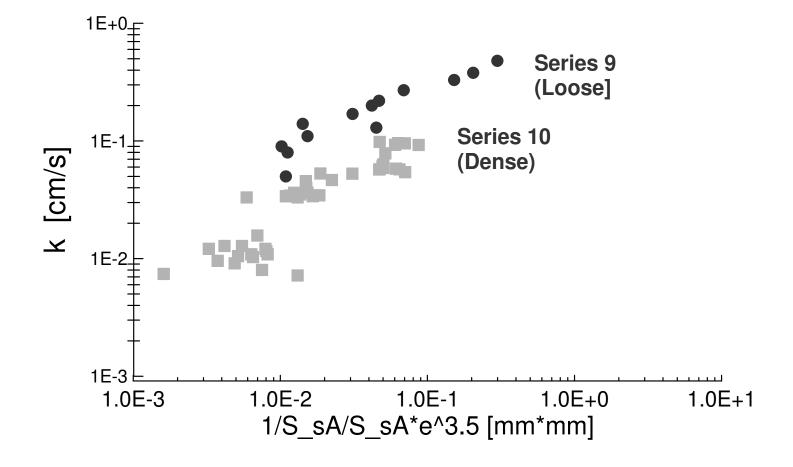


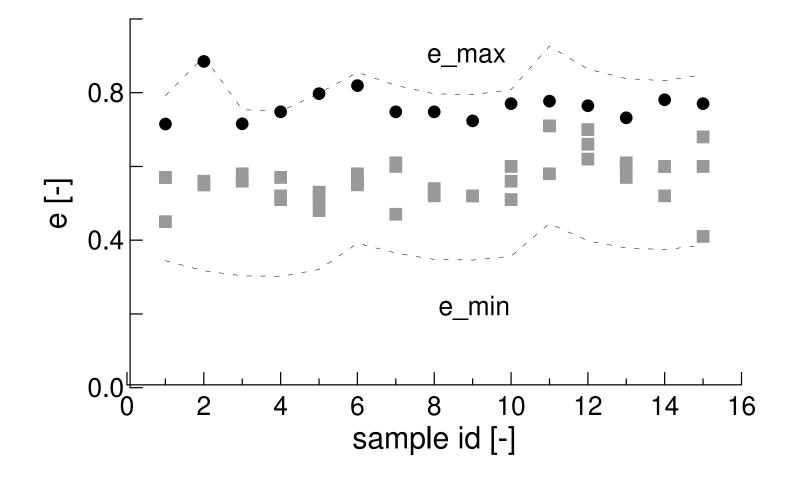


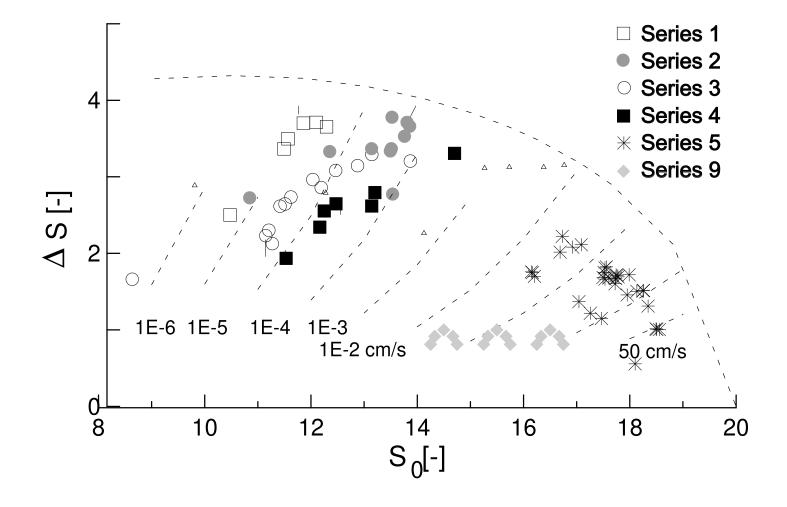


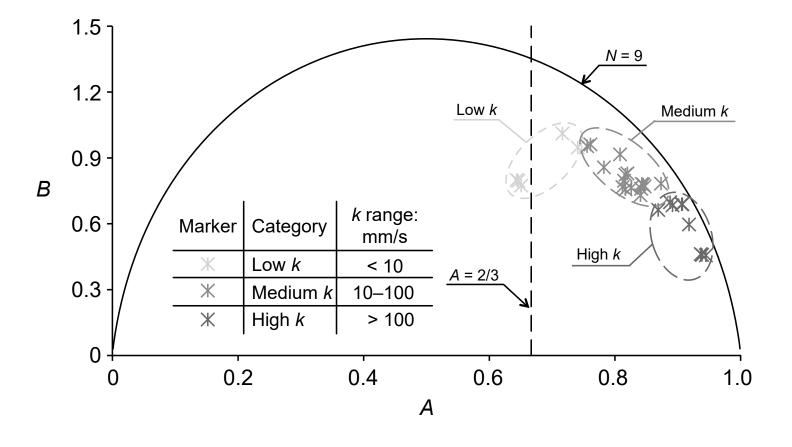












20

